

A STUDY OF REAL-TIME RECOGNITION OF UNMANNED AERIAL VEHICLES IN OUTDOOR AREAS BASED ON A RANDOM FOREST ALGORITHM

Zhoutai TIAN^{*}, Daojie YU

School of Information and Systems Engineering, Information Engineering University, Zhengzhou, Henan 450002, China

Received 4 January 2022; accepted 29 March 2022

Abstract. With the widespread use of unmanned aerial vehicles (UAVs) in life, the real-time recognition of UAVs has become an important issue. The authors of this paper mainly studied the application of the random forest (RF) algorithm in the outdoor real-time recognition of UAVs. Mel-Frequency Cepstral Coefficient (MFCC) features were extracted from sound signals firstly, and then the RF method was combined with weighted voting to obtain the improved random forest (IRF) method to identify UAV sounds and environmental sounds. An experimental analysis was conducted. The modeling time of the IRF method increased by 9.52% compared with the RF method, and the recognition rate of the IRF method decreased with the increase of the distance from the microphone; however, the recognition rate of the IRF method was always higher than that of the RF method, and the recognition rate of the IRF method for the mixed samples was always higher than 90%. When the distance was 10 m, the IRF method still had a recognition rate of 91.29%. The experimental results verify the effectiveness of the IRF method for the outdoor real-time recognition of UAVs and its practical application feasibility.

Keywords: random forest, unmanned aerial vehicle, sound signal, voting mechanism.

Introduction

An unmanned aerial vehicle (UAV) is a small aircraft with low cost, which is manipulated by wireless devices and is highly flexible and simple to operate (Wang et al., 2015). With the development of the aviation industry, UAVs have also received more and more attention, and more and more applications in the civil field (Hayat et al., 2016), such as aerial mapping (Martin et al., 2016) and agricultural monitoring (Torres-Sánchez et al., 2015), has resulted in a rapid increase in the number of UAV users. However, the current supervision of UAVs is not perfect. The arbitrary and illegal flying of UAVs have brought a series of safety problems to the society. With the popularization of UAVs, the target detection, attitude control, and recognition detection of UAVs have been widely studied. Jackson et al. (2020) conducted plant detection and mapping in Texas by UAVs at altitudes of 30, 60, and 100 m. They found that low spatial resolution (100 m altitude flight, 12 cm pixel resolution) provided less noise and more generalization capability for image classification methods. Yamazaki et al. (2020) designed a UAV human

search system combined with array microphones to detect the human body and evaluated the accuracy of the method through experiments. Zha et al. (2017) designed a nonlinear controller incorporating a trajectory linearization control (TLC) approach to control UAV attitude. They found through simulation tests that the method could well solve the common singularity problem in the current attitude control. Sapkota et al. (2016) proposed a method for online detection of small UAVs and used the AdaBoost-based method for fast object detection. They found that the method enabled accurate detection and tracking of objects. Puzanau and Nefedov (2021) studied UAV detection in a background of wind noise and designed an algorithm based on the Neyman-Pearson lemma. They found through experiments that the probability of correct UAV detection of the algorithm was 0.9 in a detection range of 200–300 m. Bao et al. (2021) established a cross-scale feature aggregation centric network to identify UAV and used a Kalman filter to track the UAV. The experiment found that the method could achieve high accuracy at a lower computational cost. Matczak and Mazurek (2021) investigated background estimation algorithms in UAV

*Corresponding author. E-mail: ttz97t@126.com

detection. They compared several background estimation algorithms, performed a Monte Carlo study, and found that the Mixture of Gaussian version 2 (MOG2) algorithm had advantages in UAV detection. Iannace et al. (2020) studied the indoor detection of UAVs. They established a model based on logistic regression to automatically detect UAVs and obtained an accuracy of 0.994 in the experiment. At present, the commonly used techniques for identifying UAVs include radar, laser, infrared, etc. Since UAVs produce large and easy-to-capture noise during flight, this paper studied the outdoor real-time identification of UAVs with a random forest (RF) algorithm based on sound signals. The extracted MFCC features were used as the input of the improved random forest (IRF) algorithm to identify UAV sounds and environmental sounds, and experiments were performed on the data set. This work aims to find a more efficient identification method for effective identification of illegally flying UAVs. This paper makes some contributions to the protection of public safety and personal privacy.

1. UAV outdoor real-time identification method

1.1. Sound signal feature extraction

The application fields of UAV can be divided into military and civilian. In military use, UAVs can excel in low-altitude reconnaissance and surveillance tasks (Yao et al., 2015) with their advantages of high concealment and survivability, and they can also perform some simple combat tasks after modification. In civilian use, UAVs can be used for disaster assessment (Al-Rawabdeh et al., 2016), environmental monitoring (Trasviña-Moreno et al., 2017; Zhou et al., 2015), etc. However, due to the low entry threshold and lack of effective control, UAVs also bring many safety problems (Birnbaum et al., 2016): (1) due to improper operation, poor signal and other reasons, UAV failure and fall can easily hurt people and damage objects; (2) the flight of UAVs may interfere with the flight of civil aircraft; (3) UAVs are difficult to be detected and intercepted, so they may be used by terrorists to threaten public safety (Lopes-Esteves et al., 2018). Therefore, the identification and detection of UAVs have become a difficult problem.

The sound of UAVs is generated by the friction between the rotor and the atmosphere, which is very different from the ambient sound. Therefore, the two sound signals can be recognized by the dichotomous classification method to achieve the purpose of real-time recognition of UAVs. Before recognition, the features of the sound signal need to be extracted first to reduce the signal dimension. The commonly used feature extraction methods are as follows.

1. Linear prediction coefficient (LPC): it is one of the earliest applied methods for sound signal feature extraction and is mainly used for speech signal processing.
2. Linear predictive cepstrum coefficient (LPCC) (Pawar & Kokate, 2021): it analyzes signals to obtain cepstrum, which has wide applications in speech recognition, and it has a high recognition rate, but requires great computational effort.

3. Mel-frequency Cepstrum Coefficient (MFCC) (Zeng et al., 2015): it is a feature extraction method based on the auditory characteristics of the human ear, which converts linear frequencies into Mel frequencies, and it has been widely used because of good discriminative performance.

In this paper, MPCC was used for feature extraction of sound signals. Using the same microphone, UAV sounds and environmental sounds are captured and converted to 5120 Hz samples in a uniform mat format. The frame and window lengths are set as 256 to extract the MFCC features of the signals. First, to improve the energy in the high-frequency region, a signal is pre-emphasized by first-order high-pass filtering. The first-order high-pass filtering is defined as follows. For a time-domain signal $x(t)$, a is set as the filtering coefficient, and the formula for its pre-emphasized output signal can be written as:

$$y(t) = x(t) - ax(t-1), 0.9 \leq a \leq 1.0. \quad (1)$$

The signal is then windowed using the Hamming window, and the calculation equation of the Hamming window can be written as:

$$w(n) = 0.54 - 0.46 \cos\left(\frac{2\pi n}{N-1}\right), 0 \leq n \leq N-1, \quad (2)$$

where N refers to the width of the window function, i.e., the frame, 256 or 512 usually.

After the above processing, the signal is then subjected to fast Fourier transform (FFT) to obtain the distribution of frequency components of the signal. The formula of FFT for the signal is:

$$F(\omega) = \int_{-\infty}^{\infty} f(t)e^{-j\omega t} dt, \quad (3)$$

where ω refers to frequency and t refers to time.

After FFT, the spectrum of every frame of the signal is written as:

$$R(f) = FFT[y(t)w(n)]. \quad (4)$$

Then, through the Meier filter, the signal is converted from the frequency domain to the Mel domain. The frequency distribution information under the Mel scale is written as:

$$F_{mel}(f) = 1125 \ln\left(1 + \frac{f}{700}\right). \quad (5)$$

The signal is processed using a set of triangular filters, and the frequency response of every filter is written as:

$$H_m(k) \begin{cases} 0, k < f_{mel}(m-1) \\ \frac{k - f_{mel}(m-1)}{f_{mel}(m) - f_{mel}(m-1)}, f_{mel}(m-1) \leq k \leq f_{mel}(m) \\ \frac{f_{mel}(m-1) - k}{f_{mel}(m+1) - f_{mel}(m)}, f_{mel}(m) \leq k \leq f_{mel}(m+1) \\ 0, k > f_{mel}(m+1) \end{cases}, \quad (6)$$

where $f_{mel}(m)$ refers to the center frequency of the m -th triangular filter under the Mel scale. Then, the logarithmic energy of every filter is calculated:

$$p(m) = \ln \left(\sum_{k=0}^{N-1} |R(k)|^2 H_m(k) \right), \quad (7)$$

Finally, the discrete cosine transform is used to obtain the cepstrum coefficient of $p(m)$:

$$c(i) = \sum_{m=0}^{M-1} p(m) \cos \left(\frac{\pi i(m-0.5)}{M_{mel}} \right), i=1,2,\dots,I_{num}, \quad (8)$$

where I_{num} refers to the order of the MFCC feature, 2–13 usually.

In the final extracted MFCC features, in addition to the cepstral coefficient calculated by the above equation, the dynamic features need to be extracted to enable a better representation of the sound signal, i.e., to find the difference of the data frame:

$$d(t) = \frac{c(t+1) - c(t-1)}{3}. \quad (9)$$

The final obtained MFCC features include 12 dimensions of cepstrum coefficients and first-order and second-order differences of cepstrum coefficients, totally 36 dimensions.

1.2. Random forest algorithm

The RF algorithm is a combinatorial classifier (Belgiu & Drăguț, 2016). It uses a classification and regression tree (CART) as a meta-classifier, combines a certain number of CARTs by the Bagging method, aggregates the classification results of CARTs (Biau & Scornet, 2015), and decides the optimal classification result through a voting mechanism. The basic concepts of the RF algorithm include CART and the Bagging method.

(1) CART: CART takes Gini index as the splitting criterion, and its calculation formula is:

$$GINI(t) = 1 - \sum_{j=1}^k [p(j|t)]^2, \quad (10)$$

where k refers to types of classes and $p(j|t)$ is the probability that class j is at node t . CART calculates the Gini index of every feature and finds out the feature with the minimal Gini index as the splitting feature to divide samples.

(2) The Bagging method: the Bagging method is an integrated feature for processing training sets. For a data set containing n samples, n' data are independently and randomly selected to generate multiple independent, autonomous training data sets. A sub-classifier is obtained after training with one training set.

The specific steps of the RF algorithm are as follows.

1. In the training sample set, k bootstrapping sample sets are generated by the Bagging method.
2. Based on the sample set, k classification trees are generated, and node splitting is performed according to the CART method without pruning the trees.
3. Multiple CARTs are built to predict unknown sam-

ples, and the predicted results are determined according to the simple voting method.

As an integrated learning algorithm, the RF algorithm has better classification performance and faster training compared with a single classifier and has been very widely used in image recognition (Hu et al., 2017), data prediction (Koreen & Murray, 2015), etc. However, the voting mechanism in the algorithm assigns the same weight to every CART, and it is impossible to separate CARTs with high and low accuracy, which affects the final classification result. In this paper, an IRF algorithm was designed for the above drawback based on the weighted voting method. Suppose that there is a test sample set X , a trained CART set T , and a classification result set C . The out-of-bag (OOB) data of decision tree t is denoted as O_t . Samples in O_t are classified by t . The classification results are compared with the actual classification, and the number of samples that are correctly classified is recorded and denoted as O_{tr} . Then, the classification accuracy of decision tree t for O_t is written as:

$$CR_t = \frac{O_{tr}}{O_t}. \quad (11)$$

The larger the value of CR_t is, the higher the accuracy of decision tree t is. CR_t is taken as the weight of decision tree t . In the final vote, the total number of votes for class c is recorded as S_c , and its calculation formula is written as:

$$S_c = \sum_{t=1}^T (T_{c,x}(x) CR_t). \quad (12)$$

When sample x belongs to class c , $T_{c,x}(x) = 1$, otherwise $T_{c,x}(x) = 0$. Then, the class with the highest number of votes is used as the final classification result of sample x :

$$C_x = \arg \max (S_c). \quad (13)$$

After the MFCC features are extracted, the UAV sound samples are marked as positive samples and denoted as 1, and the ambient sound samples are marked as negative samples and denoted as 0. Then, different samples are classified by the IRF algorithm to recognize UAVs.

2. Experimental analysis

Experiments were conducted in a MATLAB environment. Python 3.5 was used for programming. Since there might be some differences in the sound of different UAVs, to ensure the diversity of samples, three types of UAVs were used, namely, DJI Mavic 3, DJI Air 2S and DJI Mini 2. Different sounds were collected when the microphone was 1 m, 2 m, 5 m away. The distance was taken as the variable to understand the effect of microphone distance on the recognition performance. The acquisition device was the AVLE AW-818 microphone. The signal was amplified by an amplifier and then acquired using an Agilent DSO9404A oscilloscope. The extracted UAV sounds and ambient sounds were composed into experimental samples, and then feature extraction was performed. Every sample was extracted with 36-dimensional features as

the input of the IRF algorithm. A total of 12,380 positive samples and 8,940 negative samples were obtained, 60% of which were used for the training of the IRF algorithm and 40% for experimental testing.

First, the MFCC features of the two kinds of samples were compared. The results of the feature comparison between the UAV and ambient sounds are shown in Figure 1.

It was seen from Figure 1 that there were obvious differences between the MFCC features extracted from UAV sounds and ambient sounds. In general, the amplitude of ambient sounds was larger, while the amplitude of UAV sounds was relatively smaller; the two kinds of samples were also not consistent in different dimensions. Therefore, the two sounds can be well distinguished by using MFCC features.

Computational complexity generally includes time complexity and space complexity. With the development of hardware technology, the limitation of computer storage capacity has become less influential to algorithms, so the time complexity of algorithms is more considered when analyzing the computational complexity. In the practical experimental process, to measure time complexity conveniently, it is usually represented by the time consumed by executing algorithms on the same machine. A comparison of the modeling time between RF and IRF algorithms is shown in Figure 2.

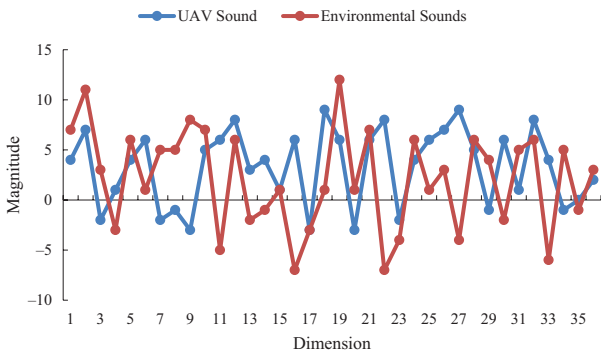


Figure 1. Comparison of MFCC characteristics between two kinds of samples

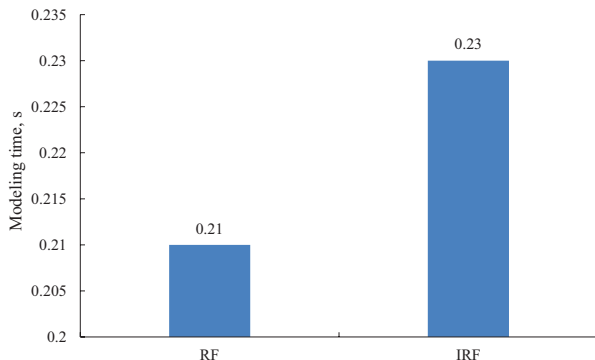


Figure 2. Comparison of the modeling time between two algorithms

It was seen from Figure 2 that the modeling time of the IRF algorithm was 9.52% longer than the RF algorithm (0.23 s vs. 0.21 s). The reason for the above result was that the IRF algorithm optimized the voting mechanism and assigned different weights to different classifiers, which led to an increase in modeling time, but the increase was not much and did not affect the efficiency of recognition too much.

Taking the distance from microphones as the variable, the recognition rates of RF and IRF algorithms for UAV sounds at different distances were compared, and the results are shown in Figure 3.

It was seen from Figure 3 that with the increase of the distance from the microphone, the recognition rate of both RF and IRF algorithms gradually decreased. When the distance was 1 m, the recognition rate of the IRF algorithm was 7.66% higher than that of the RF algorithm (97.87% vs. 90.21 %). When the distance was 10 m, the recognition rate of the RF algorithm was 75.21%, which was 15% lower than the rate when the distance was 1 m, and the recognition rate of the IRF algorithm was 90.28%, which was 7.59% lower than the rate when the distance was 1 m, but was 15.07% higher than the recognition rate of the RF algorithm at the same distance. Moreover, the recognition rate of the IRF algorithm was above 90%.

The recognition rates of RF and IRF algorithms for ambient sounds at different distances are shown in Figure 4.

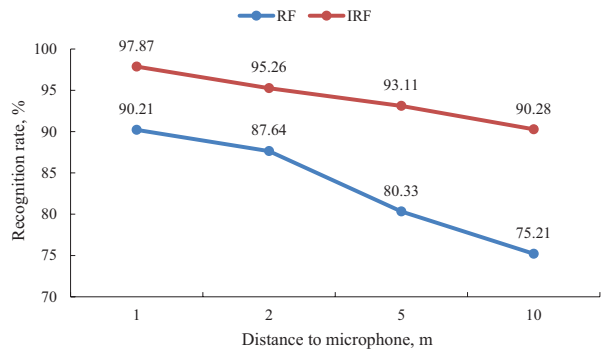


Figure 3. Comparison of UAV sound recognition rates at different distances

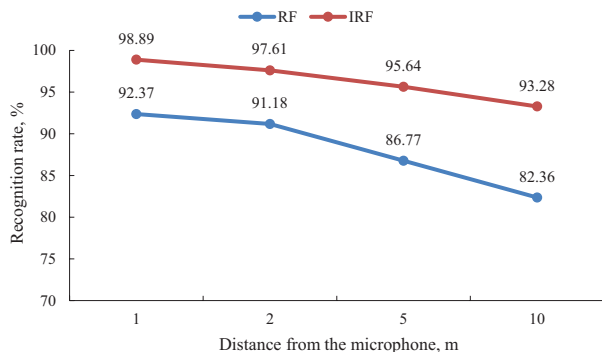


Figure 4. Comparison of ambient sound recognition rates at different distances

Table 1. Comparison of recognition rates between the two algorithms ($n = 8528$)

Distance from the microphone, m	The RF algorithm		The IRF algorithm	
	Number of samples correctly recognized	Recognition rate, %	Number of samples correctly recognized	Recognition rate, %
1	8021	94.05	8324	97.61
2	7894	92.57	8189	96.02
5	7532	88.32	7888	92.50
10	7018	82.29	7785	91.29

It was seen from Figure 4 that similar to the recognition of the UAV sound, the recognition rate of the ambient sound decreased gradually with the increase of distance from the microphone, The recognition rate of the RF algorithm was above 80% and that of the IRF algorithm was above 90%. When the distance from the microphone was 10 m, the recognition rate of the IRF algorithm was 10.92% higher than that of the RF algorithm (93.28% vs. 82.36%). The results showed that the recognition performance of the IRF algorithm was better than that of the RF algorithm.

Finally, all samples were mixed for recognition. The recognition rates of the two algorithms at different distances are shown in Table 1.

It was seen from Table 1 that the recognition rate of the two algorithms decreased gradually as the distance from the microphone increased; the algorithms had the highest recognition rates, 94.05% and 97.61% when the distance was 1 m, and the recognition rates were 82.29% and 91.29% when the distance was 10 m. In general, the recognition rate of the IRF algorithm was always higher than that of the RF algorithm, which verified that the improved IRF algorithm was reliable and could recognize UAVs effectively.

3. Discussion

With the progress of computer technology and the development of intelligent algorithms, more and more algorithms have been well applied in various fields of people's lives. Ran et al. (2021) developed a novel K-means clustering algorithm based on noise algorithm for the urban congestion problem to capture urban hotspots. They found that the method could accurately obtain clustering results and effectively capture urban hotspots through experiments on five taxi GPS datasets from Aracaju (Brazil), San Francisco (USA), Rome (Italy), Chongqing (China), and Beijing (China). Cui et al. (2021) proposed a new fault diagnosis method based on variational modal decomposition (VMD) and maximum correlation kurtosis deconvolution (MCKD) to solve the problem of weak fault signals in rolling element due to long transmission paths and found through simulation experiments that the method could effectively and accurately diagnose rolling element faults in rolling bearings. Wu et al. (2020) proposed a novel self-paced dynamic infinite mixture model

to infer the dynamics of electroencephalogram fatigue signals. They found through experiments that the proposed model showed better performance in automatically identifying the brain workload of pilots. This paper focuses on the application of RF algorithm in UAV identification.

The experimental results of this paper showed that the MFCC features could help distinguish between UAV sounds and ambient sounds, indicating that the MFCC features were reliable. The comparison between the RF algorithm and the IRF algorithm found that the modeling time of the IRF algorithm only increased by 9.52%, but the optimization did not significantly increase the calculated amount. The recognition results of UAVs suggested that the recognition rate of the algorithm for both UAV sounds and ambient sounds decreased gradually as the distance from the microphone increased; but it was found from the comparison in Table 1 that the IRF algorithm had a higher recognition rate than the traditional RF algorithm, and its recognition rate was 97.61% when the distance from the microphone was 1 m, which was 3.56% higher than that of the RF algorithm. The above results verified the effectiveness of the IRF algorithm.

Despite some achievements in the study of the outdoor real-time recognition of UAVs in this paper, there are some shortcomings. In the future work, the following needs to be carried out:

- 1) studying different UAV models to understand the applicability of the IRF algorithm;
- 2) studying the real-time recognition of multiple UAVs to improve the existing algorithm;
- 3) expanding the recognition distance to study the maximum effective detection distance of the algorithm for UAVs.

Conclusions

This paper studied the outdoor real-time recognition method of UAVs. Based on sound signals, the RF algorithm was improved. The IRF algorithm was used to capture sound signals for experimental analysis. The results demonstrated that the modeling time of the IRF algorithm was slightly longer than the RF algorithm, and the recognition rate of both algorithms decreased with the increase of the distance from the microphone, but the recognition rate of the IRF algorithm was always better than the RF algorithm. In the recognition of all samples,

the recognition rate of the IRF algorithm was above 90%, up to 97.61%, which verified the effectiveness of the IRF algorithm in the outdoor real-time recognition of UAVs. The IRF algorithm can be further promoted and applied in practice.

Author contributions

ZTT contributed the central idea, analyzed most of the data, and wrote the initial draft of the paper. DJY contributed to refining the ideas, carrying out additional analyses, and finalizing this paper.

Disclosure statement

The authors declare that he has no competing interest to report.

References

- Al-Rawabdeh, A., He, F. N., Mousa, A., El-Sheimy, N., & Habib, A. (2016). Using an unmanned aerial vehicle-based digital imaging system to derive a 3D point cloud for landslide scarp recognition. *Remote Sensing*, 8(2), 95. <https://doi.org/10.3390/rs8020095>
- Bao, M., Urgessa, G. C., Xing, M., Han, L., & Chen, R. (2021). Toward more robust and real-time unmanned aerial vehicle detection and tracking via cross-scale feature aggregation based on the center keypoint. *Remote Sensing*, 13(8), 1416. <https://doi.org/10.3390/rs13081416>
- Belgiu, M., & Drăguț, L. (2016). Random forest in remote sensing: A review of applications and future directions. *ISPRS Journal of Photogrammetry and Remote Sensing*, 114, 24–31. <https://doi.org/10.1016/j.isprsjprs.2016.01.011>
- Biau, G., & Scornet, E. (2015). A random forest guided tour. *Test*, 25(2), 1–31. <https://doi.org/10.1007/s11749-016-0481-7>
- Birnbaum, Z., Dolgikh, A., Skormin, V., O'Brien, E., Muller, D., & Stracquodaine, C. (2016). Unmanned aerial vehicle security using recursive parameter estimation. *Journal of Intelligent & Robotic Systems*, 84(1–4), 107–120. <https://doi.org/10.1007/s10846-015-0284-1>
- Cui, H., Guan, Y., & Chen, H. (2021). Rolling element fault diagnosis based on VMD and sensitivity MCKD. *IEEE Access*, 9, 120297–120308. <https://doi.org/10.1109/ACCESS.2021.3108972>
- Hayat, S., Yanmaz, E., & Muzaffar, R. (2016). Survey on unmanned aerial vehicle networks for civil applications: A communications viewpoint. *IEEE Communications Surveys & Tutorials*, 18(4), 2624–2661. <https://doi.org/10.1109/COMST.2016.2560343>
- Hu, X., Belle, J. H., Meng, X., Wildani, A., Waller, L. A., Strickland, M. J., & Liu, Y. (2017). Estimating PM_{2.5} concentrations in the conterminous United States using the random forest approach. *Environmental Science & Technology*, 51(12), 6936. <https://doi.org/10.1021/acs.est.7b01210>
- Iannace, G., Ciaburro, G., & Trematerra, A. (2020). Acoustical unmanned aerial vehicle detection in indoor scenarios using logistic regression model. *Building Acoustics*, 28(1). <https://doi.org/10.1177/1351010X20917856>
- Jackson, M. R., Portillo-Quintero, C., Cox, R. D., Ritchie, G., Johnson, M., Humagain, K., & Subedi, M. (2020). Season, classifier, and spatial resolution impact honey mesquite and yellow bluestem detection using an unmanned aerial system. *Rangeland Ecology & Management*, 73(5), 658–672. <https://doi.org/10.1016/j.rama.2020.06.010>
- Koreen, M., & Murray, R. (2015). On the importance of training data sample selection in random forest image classification: A case study in Peatland ecosystem mapping. *Remote Sensing*, 7(7), 8489–8515. <https://doi.org/10.3390/rs70708489>
- Lopes-Esteves, J., Cottais, E., & Kasmi, C. (2018). Software instrumentation of an unmanned aerial vehicle for HPEM effects detection. In *Proceedings URSI Atlantic Radio Science Conference (URSI AT-RASC)* (pp. 1–4). IEEE. <https://doi.org/10.23919/URSI-AT-RASC.2018.8471395>
- Martin, P. G., Payton, O. D., Fardoulis, J. S., Richards, D. A., Yamashiki, Y., & Scott, T. B. (2016). Low altitude unmanned aerial vehicle for characterising remediation effectiveness following the FDNPP accident. *Journal of Environmental Radioactivity*, 151(Part 1), 58–63. <https://doi.org/10.1016/j.jenvrad.2015.09.007>
- Matczak, G., & Mazurek, P. (2021). Comparative Monte Carlo analysis of background estimation algorithms for unmanned aerial vehicle detection. *Remote Sensing*, 13(5), 870. <https://doi.org/10.3390/rs13050870>
- Pawar, M. D., & Kokate, R. D. (2021). Convolution neural network based automatic speech emotion recognition using Mel-frequency Cepstrum coefficients. *Multimedia Tools and Applications*, 80(10), 15563–15587. <https://doi.org/10.1007/s11042-020-10329-2>
- Puzanau, A. D., & Nefedov, D. S. (2021). Synthesis of algorithm of unmanned aerial vehicle detection by acoustic noise. *Doklady BGUIR*, 19(2), 65–73. <https://doi.org/10.35596/1729-7648-2021-19-2-65-73>
- Ran, X., Zhou, X., Lei, M., Tepsan, W., & Deng, W. (2021). A novel K-Means clustering algorithm with a noise algorithm for capturing urban hotspots. *Applied Sciences*, 11(23), 11202. <https://doi.org/10.3390/app112311202>
- Sapkota, K. R., Roelofsen, S., Rozantsev, A., Lepetit, V., Gillet, D., Fua, P., & Martinoli, A. (2016). Vision-based Unmanned Aerial Vehicle detection and tracking for sense and avoid systems. In *IEEE/RSJ International Conference on Intelligent Robots and Systems (IROS)* (pp. 1556–1561). IEEE. <https://doi.org/10.1109/IROS.2016.7759252>
- Torres-Sánchez, J., López-Granados, E., Serrano, N., Arquero, O., & Peña, J. M. (2015). High-Throughput 3-D monitoring of agricultural-tree plantations with unmanned aerial vehicle (UAV) technology. *PLoS ONE*, 10(6), e0130479. <https://doi.org/10.1371/journal.pone.0130479>
- Trasviña-Moreno, C. A., Blasco, R., Marco, Á., Casas, R., & Trasviña-Castro, A. (2017). Unmanned aerial vehicle based wireless sensor network for marine-coastal environment monitoring. *Sensors*, 17(3), 460. <https://doi.org/10.3390/s17030460>
- Wang, X., Wang, M., Wang, S., & Wu, Y. (2015). Extraction of vegetation information from visible unmanned aerial vehicle images. *Transactions of the Chinese Society of Agricultural Engineering*, 31(5), 152–159.
- Wu, E. Q., Zhou, M. C., Hu, D. W., Zhu, L. J., Tang, Z. R., Qiu, X. Y., Deng, Y. P., Zhu, L. M., & Ren, H. (2020). Self-paced dynamic infinite mixture model for fatigue evaluation of pilots' brains. *IEEE Transactions on Cybernetics*, 52(7), 1–16. <https://doi.org/10.1109/TCYB.2020.3033005>
- Yamazaki, Y., Premachandra, C., & Perea, C. J. (2020). Audio-processing-based human detection at disaster sites with unmanned aerial vehicle. *IEEE Access*, PP(99), 1–1. <https://doi.org/10.1109/ACCESS.2020.2998776>

- Yao, P., Wang, H., & Su, Z. (2015). Real-time path planning of unmanned aerial vehicle for target tracking and obstacle avoidance in complex dynamic environment. *Aerospace Science & Technology*, 47, 269–279.
<https://doi.org/10.1016/j.ast.2015.09.037>
- Zeng, Y. C., Chen, Y. Y., Mao, Y. H., & Xie, X. J. (2015). Mel frequency cepstrum coefficient extraction method based on empirical mode decomposition and combined spectrum of Fourier transform and Wigner distribution. *Natural Science Journal of Xiangtan University*, 132(5), 563–573.
- Zha, C., Ding, X., Yu, Y., & Wang, X. (2017). Quaternion-based nonlinear trajectory tracking control of a quadrotor unmanned aerial vehicle. *Chinese Journal of Mechanical Engineering*, 30, 77–92.
<https://doi.org/10.3901/CJME.2016.1026.127>
- Zhou, H., Kong, H., Wei, L., Creighton, D., & Nahavandi, S. (2015). Efficient road detection and tracking for unmanned aerial vehicle. *IEEE Transactions on Intelligent Transportation Systems*, 16(1), 297–309.
<https://doi.org/10.1109/TITS.2014.2331353>